Digitally Controlled Boost PFC Converters operated in Mixed Conduction Mode

Koen De Gussemé, *Member, IEEE*, David M. Van de Sype, *Member, IEEE*, Alex P. Van den Bossche, *Senior Member, IEEE*, and Jan A. Melkebeek, *Senior Member, IEEE*.

***Abstract*— In this paper, the digital control of a boost power factor correction (PFC) converter operated in the mixed conduction mode is presented. The problems tackled are the input current distortion due to oscillation of parasitic components, the erroneous sampling of the input current in the discontinuous conduction mode, and eventually, the input current distortion due to the change in converter dynamics. The first problem can be solved by using a snubber, while the other two problems are solved by extending the control algorithm with sample correction and duty-ratio feedforward.**

***Index Terms*— Boost Converter, Power Factor Correction, Digital Control**

I. Introduction

SO as to supply DC-applications from the AC-grid with low harmonic content of the input current, power factor correction (PFC) converters, consisting of a bridge rectifier and a switching DC-DC converter, are employed. For low power applications, DC-DC converters like buck, boost, buck-boost, SEPIC or Ćuk converters are often operated in discontinuous conduction mode (DCM), allowing easy control of the input current waveform [1], [2]. Nevertheless, due to high device stresses and problems with conducted emission, this approach must be abandoned when higher power is required.

he most popular topology for high power applications is the boost converter, operated in continuous conduction mode (CCM) [3]–[5]. Fig. 1 shows the basic topology of the boost PFC converter. When the switch S is conducting, the input current i_L will rise, increasing the energy stored in the inductor L. When the switch is turned off, the current will flow through diode D and the energy of the inductor will be transferred towards the output capacitor. During the off-time of the switch, the input current will decrease until the start of the next on-time (CCM, Fig. 3), or until the input current becomes zero (DCM, Fig. 4). The operation mode (CCM or DCM) of the converter is depending on the converter parameters. In general, for a given converter, CCM will occur when the converter is operated at high input current, DCM at low input current. Since for PFC the input current waveform is forced to be proportional to the input voltage in order to obtain a resistive input, the average input current will be nearly sinusoidal. As a result, it is possible that both conduction modes occur alternately, see Fig. 2. This operating mode will be called mixed conduction mode (MCM) [6], [7].

All authors are with the Electrical Energy Lab (EELAB), Department of Electrical Energy, Systems and Automation (EESA), Ghent University, Sint-Pietersnieuwstraat 41, B-9000 Gent, Belgium. Phone: +32 9 264 3420, Fax: +32 9 264 3582, E-mail: degusseme@eesa.ugent.be

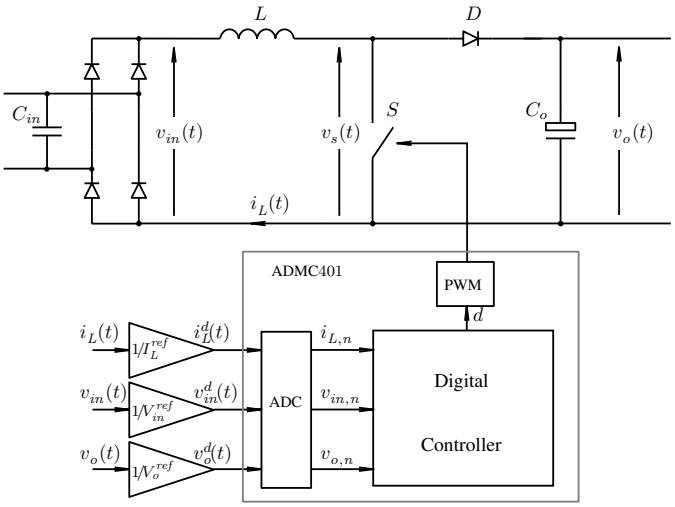

Fig. 1. A digitally controlled boost PFC converter

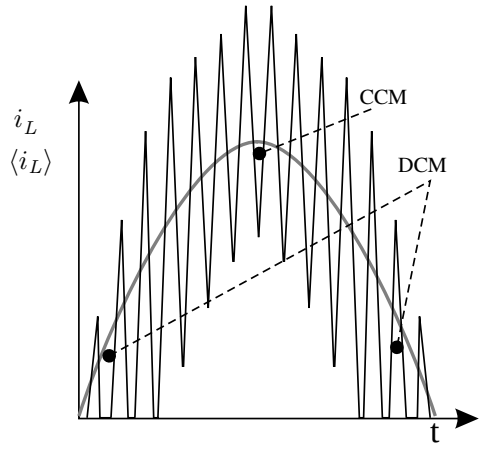

Fig. 2. The input current of a boost PFC converter operated in MCM

When boost PFC converters, designed for operation in CCM, are operated at low power, implying operation in MCM or even DCM during the entire grid period, the input current waveform will become distorted, and the amount of harmonics in the input current will rise dramatically. Reasons are parasitic effects [8], errors in the input current sampling [7], and a sudden change in the converter dynamics [9], [10]. In [11] operation in the mixed conduction mode is avoided by changing the switching frequency for different power levels. Nevertheless, when fast load changes occur, or when low switching frequencies are undesirable, a solution is required,

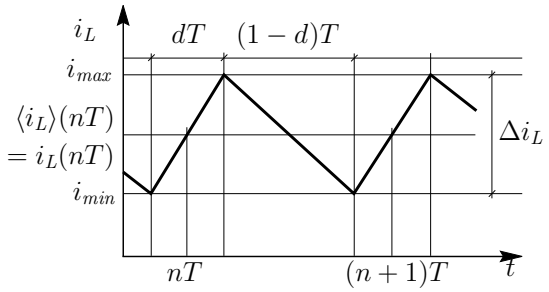

Fig. 3. Input current in CCM

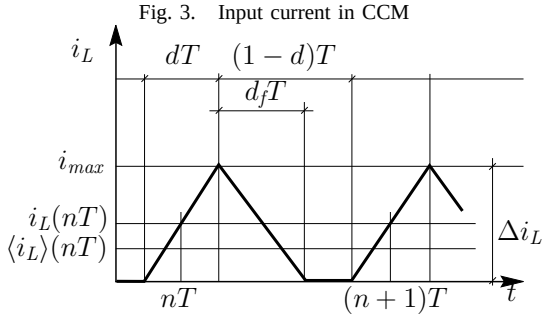

Fig. 4. Input current in DCM

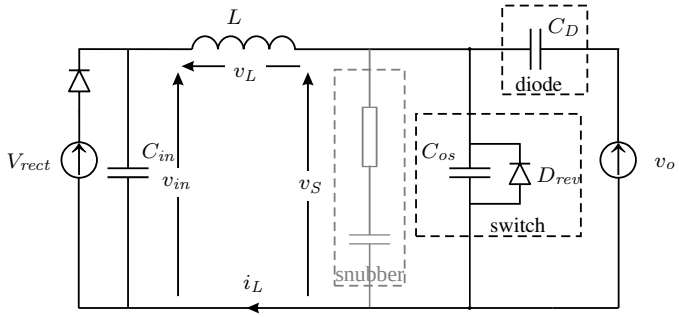

Fig. 5. Parasitic network causing oscillations in the input current, gray: snubber

which tackles the problems encountered in MCM by adapting the controller to MCM operation. The problem of parasitic oscillations can be easily reduced by inserting a snubber into the converter topology. The problems of sampling and changing converter dynamics can be solved by employing the wide range of possibilities of a digital controller. Sample correction is used to correct the erroneous sampling, while duty-ratio feedforward helps the controller to force the input current to behave resistive. All improvements are tested on a 1kW boost PFC converter. The results are a very low THD and a high power factor in the entire power range of the converter.

II. Parasitic Oscillations

A first problem which can be encountered when operating a boost converter in DCM, is the existence of parasitic oscillations on the switch voltage and the input current[8]: at the moment the inductor current becomes zero, the switch voltage should adopt the input voltage, and the input current should remain zero. Nevertheless, for real switches, a network, consisting of parasitic capacitances C_{os} of the switch and C_D of the diode, and the inductor L (Fig. 5) starts oscillating at

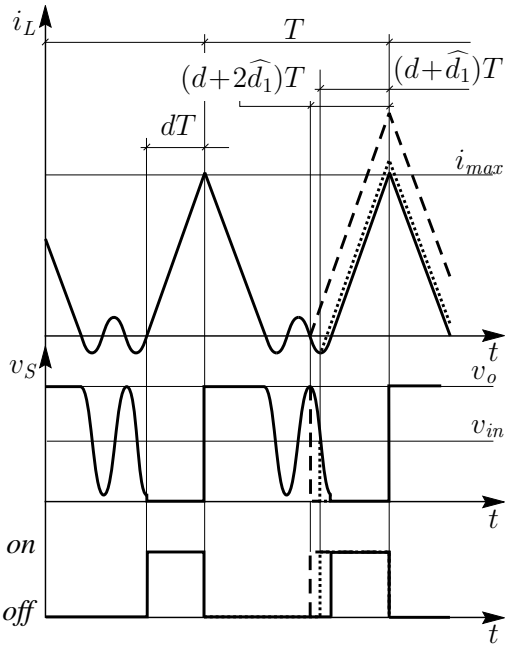

Fig. 6. Converter waveforms for two different steps in the duty-ratio

that instant (Fig. 6). The switch voltage varies between v_o and $2v_{in} - v_o$ for high values of the input voltage. The switch voltage oscillation and the inductor current oscillation can be described approximately as

$$v_S(t) = v_{in} + (v_o - v_{in}) \cos\left(\omega_n (t - t_2)\right) \tag{1}$$

$$i_L(t) = -\frac{v_o - v_{in}}{Z_n} \sin\left(\omega_n (t - t_2)\right), \tag{2}$$

with

$$\omega_n = \frac{1}{\sqrt{LC_n}} \qquad \text{and} \qquad Z_n = \sqrt{\frac{L}{C_n}}. \tag{3}$$

For low values of the input voltage, the switch voltage is first clamped to $0V$ by the reverse diode D_{rev} of the switch, before an oscillation of this network starts. The oscillation is hardly attenuated and lasts until the switch S is turned on again. As a result, the input current at the start of the next on-time of the switch can be either positive, negative or zero, depending on the phase of the oscillation.

In the case of ideal switches, the peak value i_{max} of the inductor current is proportional to the duty-ratio

$$i_{max} = \frac{dT v_{in}}{L}, \tag{4}$$

As a result, an increase of the duty-ratio will cause a proportional increase of the peak current. Nevertheless, in the case of real switches, the increase of the peak current caused by a duty-ratio step $\widehat{d}$ is not inherently proportional to the magnitude of that duty-ratio step. Fig. 6 shows clearly that, depending on the instantaneous value of the input current at the beginning of the on-time of the switch, a duty-ratio step $\widehat{d_1}$ may cause a minor increase of the input current (dotted lines), whereas an increase of the duty-ratio with $2\widehat{d_1}$ will result in a large increase of the input current (dashed lines). Consequently, the gain of the duty-ratio-to-input-current transfer function is depending on the magnitude of the step

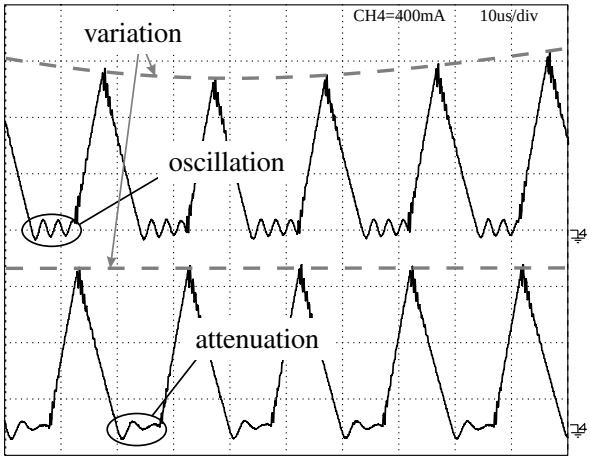

Fig. 7. Uncontrolled variation of the input current, due to oscillation of the parasitic network

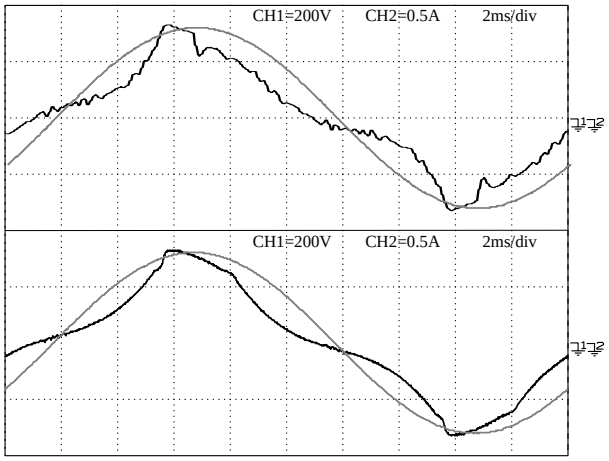

Fig. 8. Input current and input voltage waveforms of the boost PFC converter, without snubber (upper traces) and with snubber (lower traces)

in the duty-ratio, and, due to the parasitic nature of the oscillation, unpredictable. This effect results in unpredictable inductor current behavior, causing input current distortion or even inductor current loop instability.

For this problem, all solutions decreasing the amplitude of the oscillation will improve the quality of the input current waveform. The simplest solution is shown in Fig. 5: a snubber is added to attenuate the oscillation. The result is shown in the lower traces of Figs. 7 and 8.

III. Typical Control of a Boost PFC Converter in CCM

The typical control of a digitally controlled boost PFC converter uses two controllers: an output voltage controller, and an input current controller. The output voltage controller changes the desired input conductance g_e of the converter in order to keep the input and the output power of the converter balanced, resulting in a constant output voltage v_o. Since this control loop is very slow in comparison to the input current control loop, the input conductance g_e will be treated as a constant value G_e in the next sections.

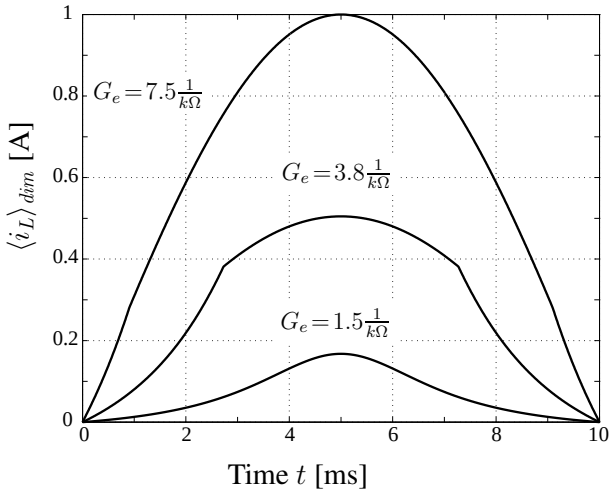

Fig. 9. Averaged input current waveforms for operation in MCM

The reference value i_L^* for the input current is obtained by multiplying G_e with the input voltage v_{in}. The output of the current loop is the duty-ratio d, which is sent to a PWM-unit to control the switch S of the boost converter. When digital control is applied, the control variables, input voltage v_{in}, output voltage v_o and the input current i_L, must be sensed, scaled and converted into digital quantities ($v_{in,n}$, $v_{o,n}$, and $i_{L,n}$ respectively). Nevertheless, in order to simplify the equations, next sections use absolute values instead of dimensionless digital quantities.

IV. Input Current Sampling

As the sampling frequency of an analog-to-digital converter (ADC) is limited and the switching of the boost converter causes a large ripple on the input current (Fig. 2), it is hard to obtain an accurate representation of the input current waveform. Moreover, the use of a lower sampling frequency will cause aliasing. Therefore, the sampling is generally synchronized with the switching of the converter, producing one sample $i_L(nT)$ each switching cycle. If this sample is taken on the middle of the rising edge of the input current (Rising Edge Sampling, RES), the sample is equal to the averaged input current $\langle i_L \rangle$ (averaged over one switching cycle), as long as the converter operates in CCM (Fig. 3) [5].

For a boost converter operating in DCM, the input current sample obtained by the RES-algorithm will overestimate the averaged input current by a factor κ [7]

$$\langle i_L \rangle(nT) = i_L(nT)\,(d + d_f) \triangleq \kappa(nT) i_L(nT), \qquad (5)$$

where dT is the length of the rising edge of the input current and $d_f T$ is the length of the falling edge of the input current. As a result, κ will be unity in CCM and less than 1 in DCM. Using the volt-seconds balance of the input inductor

$$dT v_{in} = d_f T (v_o - v_{in}), \qquad (6)$$

the ratio κ is expressed as a function of the control variables

$$\kappa(nT) = d + d_f = \frac{d v_o(nT)}{v_o(nT) - v_{in}(nT)}. \qquad (7)$$

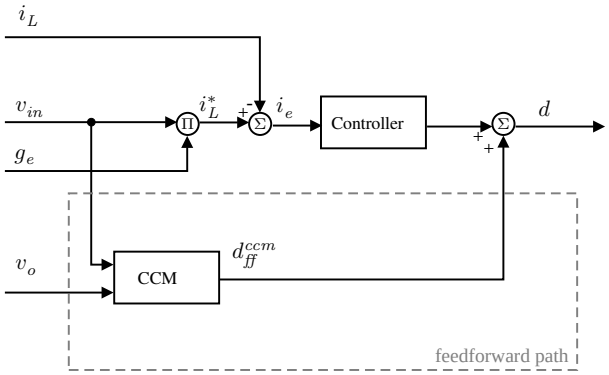

Fig. 10. Control diagram in CCM with duty-ratio feedforward

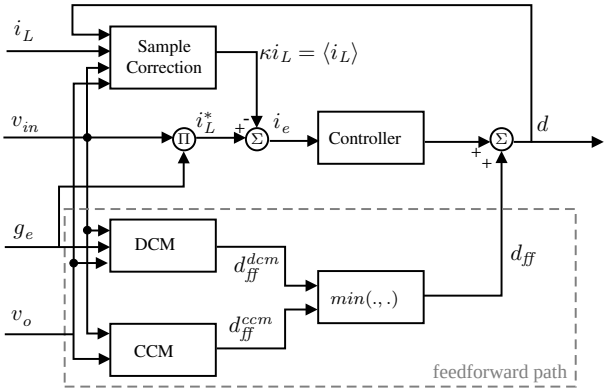

Fig. 11. Complete control diagram with sample correction and duty-ratio feedforward

Since the input current controller forces the input current samples $i_L(nT)$ to follow the reference current $G_e\widehat{V}_g|\sin(\omega t)|$ (with $\widehat{V}_g|\sin(\omega t)|$ the rectified line voltage), the averaged input current $\langle i_L \rangle$, given by (5), will be too low in DCM operation and the input current is distorted. The resulting input current waveforms for sinusoidal line voltage and a perfect input current controller can be determined by combination of (5) and (7)

$$\langle i_L \rangle(nT) = \frac{2G_eL}{T}\frac{V_o}{V_o - \widehat{V}_g|\sin(\omega nT)|}G_e\widehat{V}_g|\sin(\omega nT)|. \tag{8}$$

The input current waveform for MCM will be a combination of (8) for the DCM-part of the line period, and $G_e\widehat{V}_g|\sin(\omega t)|$ for the CCM part of the line period. The resulting waveforms are shown in Fig. 9 for different values of the input conductance (corresponding with different values of the input power).

As the ratio between the averaged input current and the input current samples can be calculated using (7) as a function of known variables (the input voltage and output voltage are sampled, while the duty-ratio is the output of the controller), the processor has all required data to calculate the correct value of the averaged input current by multiplying the input current sample $i_L(nT)$ with the ratio κ. This multiplication is also valid in CCM operation, where κ equals 1. As a result, no detection of the conduction mode is required.

V. Duty-Ratio Feedforward

When sample correction is applied, the processor will have the correct values of the averaged input current at its disposal. This yields a theoretically perfect input current waveform, under the condition of a perfect input current controller. Since the actual input current controller is designed only for CCM operation, and the duty-ratio-to-input-current transfer functions for CCM, $G_i^{ccm}(s)$, and DCM, $G_i^{ccm}(s)$, differ,

$$G_i^{ccm}(s) = \frac{\widehat{i}_L(s)}{\widehat{d}(s)} = \frac{V_o}{sL}, \tag{9}$$

and [9], [10]

$$G_i^{dcm}(s) = \frac{\widehat{i}_L(s)}{\widehat{d}(s)} = \frac{\frac{2V_o}{L}}{s + \frac{2(V_o - V_{in})}{DTV_{in}}}, \tag{10}$$

the input current will still be distorted in MCM and DCM operation.

An obvious choice to deal with changing converter parameters would be to adapt the parameters of the input current controller, usually a PI-controller, to DCM operation and change these controller parameters when the transition between the conduction modes occurs. Nevertheless, detection of this transition is difficult as the sensing and sampling of the appropriate variables (the inductor current or the input and output voltages…) may introduce some errors, and the border between continuous and discontinuous conduction mode is crossed slowly (it may take several switching cycles). This may cause the DCM controller to be active during CCM operation or vice versa. As a result, the input current waveform will remain distorted.

A possible solution is to employ duty-ratio feedforward. This control algorithm, applied before on a converter operated in CCM only [12], calculates the theoretical duty-ratio and forwards it to the output of the controller. It is displayed in Fig. 10. The ideal duty-ratio for CCM can be calculated as

$$d_{ff}^{ccm} = 1 - \frac{v_{in}}{v_o}. \tag{11}$$

One of the main features of this control algorithm is the small influence of the gain of the controller on the converter waveforms, since this controller is now only compensating for some small errors. As a result, this algorithm is very suitable to use in DCM, where the controller gain, optimized for CCM operation, is too low.

The required ideal duty-ratio for DCM can be easily obtained since the averaged input current $\langle i_L \rangle$ is directly related to the duty-ratio, yielding

$$d_{ff}^{dcm} = \sqrt{\frac{2G_eL}{T} \cdot \frac{v_o - v_{in}}{v_o}}. \tag{12}$$

Expressions (11) and (12) equal at the transition point between DCM and CCM, allowing an easy decision of the correct forwarded duty-ratio: the processor must take into account the lowest value of both. The complete control scheme including sample correction and duty-ratio feedforward is depicted in Fig. 11.

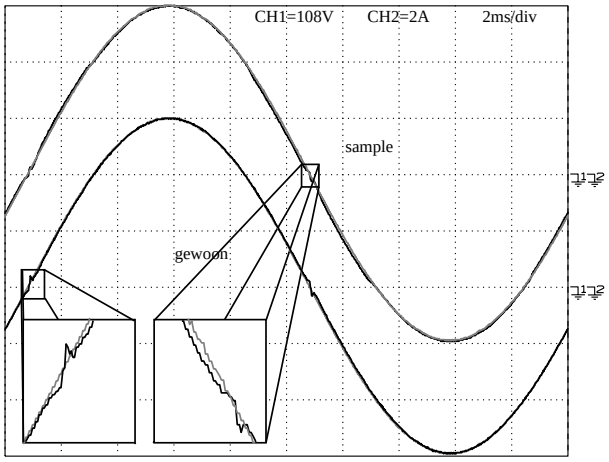

Fig. 12. Input current and input voltage waveforms of the experimental converter, with CCM-controller (lower traces), and with MCM-controller, including feedforward and sample correction (upper traces)

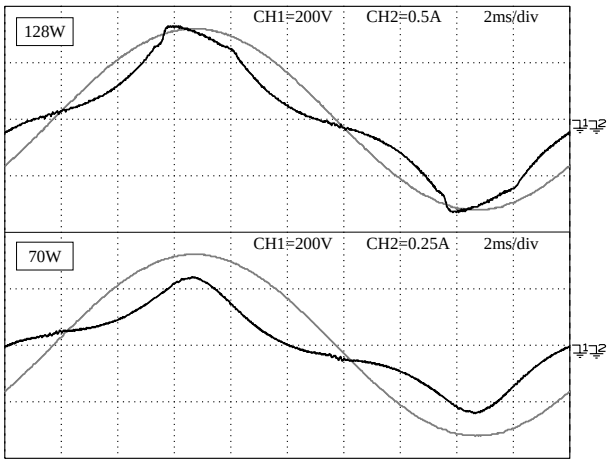

Fig. 13. Input current and input voltage waveforms for 128 and 70W programmed input power, without sample correction and duty-ratio feedforward

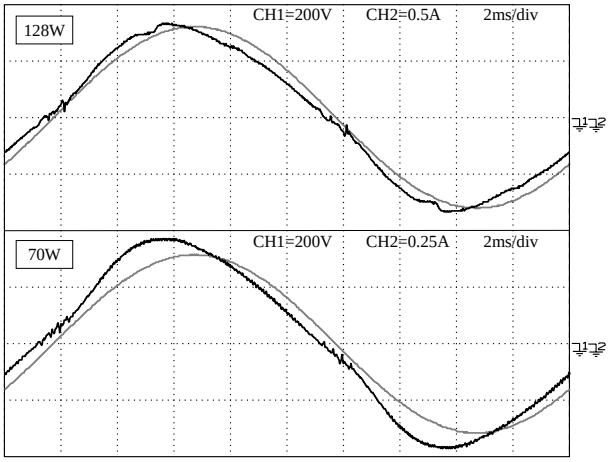

Fig. 14. Input current and input voltage waveforms for 128 and 70W programmed input power, with sample correction, and without duty-ratio feedforward

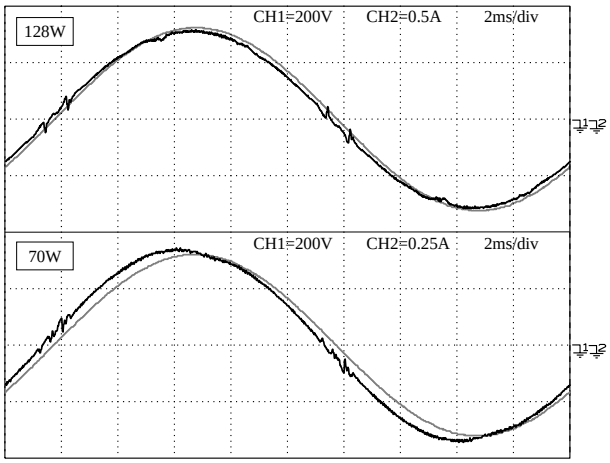

Fig. 15. Input current and input voltage waveforms for 128 and 70W programmed input power, with sample correction and duty-ratio feedforward

VI. Experimental Results

In order to verify the analysis and to test the proposed control algorithms, a 1kW boost PFC converter was build with the following converter parameters

$$\begin{cases} V_g = 230\text{V}, & f_g = 50\text{Hz}, & T = 19.6\mu\text{s} \\ V_o = 400\text{V}, & C_o = 470\mu\text{F}, & L = 1\text{mH} \end{cases} \tag{13}$$

This converter operates in the mixed conduction mode for input powers between about 100W and 500W. The improvement in the input current waveform obtained by addition of a snubber, is already demonstrated in Figs. 7 and 8. The input current waveforms of this converter at different power levels, demonstrating the operation of the new control algorithms, are displayed in Figs. 12–15. Operation at full power is shown in Fig. 12, with the input current controller of Fig. 10 (lower traces) and using the controller adapted to MCM operation (Fig. 11), including sample correction and duty-ratio feedforward for MCM (upper traces). Since the difference between the two input current waveforms is hardly noticeable, it is shown that the CCM waveforms are not affected by the sample correction. Measurement of the total harmonic distortion, and the power factor reveals only small variations: the THD remains lower than 2% in both cases, while the power factor decreases from unity to 0.999.

For operation at 128W and 70W input power, yielding MCM and DCM operation respectively, the waveforms are shown in Figs. 13–15 for three different controllers: operation with the PI-controller for CCM operation (Fig. 13), with sample correction (Fig. 14), and with both sample correction and duty-ratio feedforward (Fig. 15). The waveforms of Fig. 13 show good correspondence to the theoretical waveforms of Fig. 9. Employing sample correction leads to an important improvement of the input current waveform, for MCM as well as for DCM operation. Since the gain of the CCM PI-controller is too low to achieve good input current tracking, the addition of duty-ratio feedforward is necessary to realize another improvement in the input current waveforms. The obtained waveforms are very close to the input current waveforms. The small displacement between the input current and the input voltage, is caused by the input capacitance of the EMI-filter.

In order to quantify the improvements achieved by the new control algorithm, the total harmonic distortion (THD), and the

TABLE I

EXPERIMENTAL MEASUREMENTS OF THE THD AND THE POWER FACTOR, PI=PI-CONTROLLER, SC=SAMPLE CORRECTION, AND FF= FEEDFORWARD

P_{in}^{p}[W] $= G_e V_g^2$	THD [%]			power factor		
	PI	SC	SC+FF	PI	SC	SC+FF
252	11.1	6.5	2.4	0.991	0.993	0.999
128	26.2	7.2	2.8	0.964	0.988	0.997
70	32.6	9.1	2.8	0.926	0.976	0.992

power factor are measured in the three cases, for 252W, 128W (MCM), and 70W (DCM). The results are shown in Table I. Whereas the THD of the input current is limited to 11% for 250W input power, it increases to 32.6% for 70W input power, when no DCM-algorithm is used. Nevertheless, when employing both sample correction and duty-ratio feedforward, the THD is reduced to values lower than 3%, for the entire power range of the converter. The power factor, which is setting for low values of the programmed input power, due to the influence of the input capacitance, now remains higher than 0.99.

VII. CONCLUSION

When power factor correction converters, designed for operation in the continuous conduction mode, are operated at reduced power, operation in the discontinuous conduction mode appears near the crossover of the line voltage, or in the entire line cycle when the load is further reduced. When this occurs, the input current becomes distorted, due to parasitic oscillations, to erroneous sampling of the input current when digital control is applied, and to changing converter dynamics at the crossover between continuous and discontinuous conduction mode. The problem of parasitic oscillations can be easily reduced by inserting a snubber into the converter topology. The problems of sampling and changing converter dynamics can be solved by employing the wide range of possibilities of a digital controller. Sample correction is used to correct the erroneous sampling, while duty-ratio feedforward helps the controller to force the input current to behave resistive. All improvements are tested on a 1kW boost PFC converter. The results are a very low THD and a high power factor in the entire power range of the converter.

REFERENCES

[1] D.S.L. Simonetti, J. Sebastian, and J. Uceda, "The discontinuous conduction mode sepic and ćuk power factor preregulators: analysis and design," *IEEE Trans. Ind. Electr.*, Vol. 44, No. 5, Oct. 1997, pp. 630–637.

[2] D.S.L. Simonetti, J.L.F. Vieira, and G.C.D. Sousa, "Modeling of the high-power-factor discontinuous boost rectifiers," *IEEE Trans. Ind. Electr.*, Vol. 46, No. 4, Aug. 1999, pp. 788–795.

[3] S. Buso, P. Mattavelli, L. Rossetto, and G. Spiazzi, "Simple digital control improving dynamic performance of power factor preregulators," *IEEE Trans. Power Electr.*, Vol. 13, No. 5, Sept. 1998, pp. 814–823.

[4] A.H. Mitwalli, S.B. Leeb, G.C. Verghese, and V.J. Thottuvelil, "An adaptive digital controller for a unity power factor converter," *IEEE Trans. Power Electr.*, Vol. 11, No. 2, March 1996, pp. 374–382.

[5] D.M. Van de Sype, K. De Gussemé, and J.A.A. Melkebeek, "A sampling algortihm for digitally controlled boost PFC converters," *Proc. of the IEEE Power Electr. Spec. Conf.*, PESC 2002, June 23-27, 2002, Cairns, Australia, pp.1693-1698.

[6] J. Sebastian, J.A. Cobos, J.M. Lopera, and J. Uceda, "The determination of the boundaries between continuous and discontinuous conduction modes in pwm dc-to-dc converters used as power factor preregulators," *IEEE Trans. Power Electr.*, Vol. 10, No. 5, Sept. 1995, pp. 574–582.

[7] K. De Gussemé, D.M. Van de Sype, A.P. Van den Bossche, and J.A. Melkebeek, "Sample correction for digitally controlled boost pfc converters operating in both ccm and dcm," *Proc. of the IEEE Appl. Power Electr. Conf.*, APEC 2003, Feb. 9–13, 2003, Miami Beach, Florida, USA, pp. 389–395.

[8] K. De Gussemé, D.M. Van de Sype, A.P. Van den Bossche, and J.A. Melkebeek, "Input current distortion of ccm boost pfc converters operated in dcm," *Proc. of the IEEE Power Electr. Spec. Conf.*, PESC 2003, June 15–19, 2003, Acapulco, Mexico, pp. 1685–1690.

[9] V. Vorpérian, "Simplified analysis of pwm converters using model of pwm switch, part II: discontinuous conduction mode" *IEEE Trans. Aero. Electr. Sys.*, Vol. 26, No. 3, May 1990, pp. 497-505.

[10] J. Sun, D. Mitchell, M. Greuel, P. Krein, and R. Bass, "Averaged modeling of pwm converters operating in discontinuous conduction mode," *IEEE Trans. Power Electr.*, Vol. 16, No. 4, July 2001, pp. 482–492.

[11] R.K. Tripathi, S.P. Das, and G.K. Dubey, "Mixed-mode operation of boost switch-mode rectifier for wide range of load variations," *IEEE Trans. Power Electr.*, Vol. 17, No. 6, Nov. 2002, pp. 999–1009.

[12] D.M. Van de Sype, K. De Gussemé, A.P. Van den Bossche, and J.A. Melkebeek, "Duty-ratio feedforward for digitally controlled boost pfc converters," *Proc. of the IEEE Appl. Power Electr. Conf.*, APEC 2003, Feb. 9–13, 2003, Miami Beach, Florida, USA, pp. 396–402